Numerical investigation on the cavitating flow in Annular Jet Pump under different flow rate ratio

L Z Xiao, X P Long, Q Lyu, Y Hu, Q Q Wang
School of Power and Mechanical Engineering, Wuhan University, Hubei, 430072 China
Key Laboratory of Hubei Province for Water Jet Theory & New Technology, Hubei, 430072, China

E-mail: xplong@whu.edu.cn

Abstract. The nozzle of annular jet pump (AJP) is annular and the secondary flow is encircled by the primary flow which is of great differences with that of central jet pump (CJP). Since the high velocity working flow soaring out the annular nozzle adheres to the inner wall, the cavitation is considerably easy to be induced at the intersection of the suction chamber and the throat. This paper mainly investigated the inception and development of the cavitation in an AJP under different flow rate ratio q by numerical methods and the results was validated by the experimentation. The turbulent model is set as Realizable k-ε model, which combined with the mixture multiphase model and the Schnerr-Sauer cavitation model. The SIMPLEC algorithm is applied to solve the coupling of pressure and velocity. The simulated results confirms well with experimental data. As the working condition varies, specifically when the pressure of the outlet decreases to a certain value, the intersection of the suction chamber and the throat sees the inception and development of the cavitation and the bubble generates there adheres to the inner wall. With the decreasing outlet pressure, the cavitation region expands to the diffuser along the inner wall, and also to the axis. When the cavitation region develops to the axis and the pressure there reaches to the critical cavitation pressure (generally vapor pressure), the pump turns into the operation limits and the efficiency drops abruptly. Furthermore, when the flow rate ratio q is considerably low (generally <0.2), the shearing layer and the center of the recirculation also experience the cavitation inception. It is for this reason that the relationship between the critical cavitation number σ_c and the cavitation flow rate ratio q_c can be divided into two parts. When σ_c<0.31, it varies little with the increasing q_c, while it increases linearly with the increasing q_c when ranging from 0.31 to 1.58.

1. Introduction

Being different from central jet pump (CJP), annular jet pump (AJP), in which the flow resembles the confined annular jet, is a jet pump with an annular nozzle encircling the suction pipe. It is because the suction pipe is surrounded by the nozzle on the axis that AJP is suitable to convey the liquid containing large solid particles, such as potato, onion and capsule, even the live fish. Nevertheless, since the high pressure working flow is running adhering to the inner wall; cavitation can be induced at the intersection of the suction chamber and the throat. As the outlet pressure is decreasing, the cavity will develop and extend in the throat with the bubbles conveyed downstream, while the pump performance varies little. However, when the outlet pressure drops to a critical value, the cavitation in

the throat boosts with large amounts of cavitation cloud come into being and the pump performance experiences a sudden decrease.

There are relatively little studies on AJP. Shimizu et al. [1][2] conducted a series of experiments on 25 AJPs with different area ratios, throat length and inclined angle of the suction chamber, and the variation of the cavitation performance in AJP was obtained. Elger et al. [3] investigated the size and position of recirculation in gas AJP under different area ratio and he confirmed the onset and disappearance of the recirculation through a dimensionless number J (the momentum ratio of the primary flow and secondary flow). In addition, Long et al. [4] did some researches on the optimum structural design of AJP.

As for the cavitation flow in jet pump, there are numerous studies for CJP [5]-[8], while little for AJP. Kudirka and Decoster [6] suggested that the vapor bubble firstly occured inside the jet boundary and they suggested that the jet pump was substantially less susceptible to cavitation at 280℃ than at 80℃. Pan and Katz [9] presented that the cavitation inception appearing at the vortex centre was due to the fluctuation of the shearing layer, and it also formed in the vortex centre of the co-flow with the cavitation nuclei growing,. Ignoring the surface tension and heat transfer, Wiesche [7] analysed the cavitation behind the obstacles in an automotive fuel jet pump and simulated the cavitation phenomenon through VOF model combined with the k-ε model. Resorting to the experimentation, Long et al. [8] observed the cavitation inception at the shearing layer of the jet with several bubbles forming there, and he also captured the liquid-vapor mixing shock wave under the limited operation condition.

However there is little investigation on the cavitation inception and development in AJP. There are not consentaneous conclusions on the mechanism of the cavitation inception in AJP and the corresponding development process is not clear. Thus, through numerical method, this work devotes to investigating the inception and development of cavitation flow in the AJP under different flow rate ratio and outlet pressure.

2. Simulation Strategy

2.1. Numeric model and strategy

As shown in Fig. 1, a typical AJP is mainly comprised of annular nozzle, suction pipe, suction chamber, throat, diffuser and outlet pipe. The high pressure working flow (Primary flow) soars into the suction chamber through the annular nozzle, and then exerts a great entrainment to the secondary flow. After mixing intensively in the throat, the two flows are pumped out through the diffuser and outlet pipe. Within this procedure, the pressure of the secondary flow increases gradually.

In this paper, the tested AJP in reference [2] was chosen as the simulating prototype. The dimensions are specifically shown as follows: D_0=55mm, D_{s0}=43mm, D_t=38mm, α=18°, L_t/D_t=2.69, β=5.8°, area ratio m=1.75, nozzle thickness t=2mm.

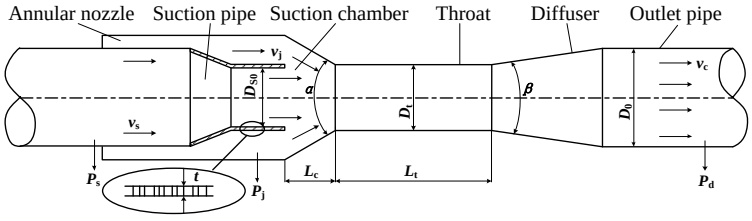

Fig. 1 configurations of AJP

The flow inside AJP can be assumed to be confined axial symmetric flow, so the 2-demensional axial symmetric model was adopted to minimize the calculating load. The calculation domain and the grid details at the suction chamber were shown in Fig. 2. As shown in the figure, the original point was set at the outlet of the suction pipe. The primary and secondary flow, accompanied with energy transfer, will mix intensively in the suction chamber and the cavitation inception appeared there firstly, hence the mesh at the corresponding place was refined.

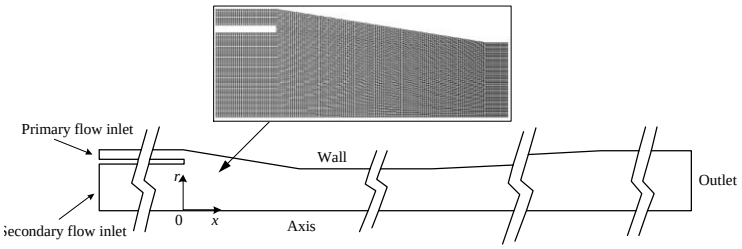

Fig. 2 Calculation domain and grid details of the pump CFD model

When the pump encounters the cavitation, the inner flow of AJP is unsteady incompressible liquid-gas two phase flow. Therefore, the unsteady model was chosen in this work. According to the previous investigation [10], Realizable *k-ε* model is suitable to simulate the cavitation flow in jet pump and it is also utilized in this work. In addition, the multi-phase model and cavitation model are respectively set as Mixture model and Schnerr-Sauer model.

As for the vapor/liquid two-phase mixture model, the fluid was assumed to be homogeneous, so the multiphase fluid components are assumed to share the same velocity and pressure. The continuity and momentum equations for the mixture flow are

$$\frac{\partial \rho_m}{\partial t}+\frac{\partial\left(\rho_m u_j\right)}{\partial x_j}=0 \tag{1}$$

$$\frac{\partial\left(\rho_m u_i\right)}{\partial t}+\frac{\partial\left(\rho_m u_i u_j\right)}{\partial x_j}=-\frac{\partial p}{\partial x_i}+\rho_m f_i+\frac{\partial}{\partial x_j}\left[\left(\mu+\mu_t\right)\left(\frac{\partial u_i}{\partial x_j}+\frac{\partial u_j}{\partial x_i}-\frac{2}{3}\frac{\partial u_k}{\partial x_k}\delta_{ij}\right)\right]. \tag{2}$$

where u_i and f_i are the velocity and body force in *i* direction, p is the mixure pressure, μ and μ_t are the laminar viscosity and the turbulent viscosity respectively. The mixture density is defined as:

$$\rho_m=\alpha_v\rho_v+\left(1-\alpha_v\right)\rho_l. \tag{3}$$

where α_v is the volume fraction of vapor. ρ_l and ρ_v are the density of liquid and vapor. The correlation of α_v and the number of bubbles per volume of liquid n_b can be obtained through the following equiation:

$$\alpha_v=\left(n_b\frac{4}{3}\pi R_B^3\right)/\left(1+n_b\frac{4}{3}\pi R_B^3\right). \tag{4}$$

where n_b is set as a constant, 1e+13. R_B is bubble radius. When cavitation emerges, the control equations for mass transfer is

$$\frac{\partial}{\partial t}\left(\alpha_v\rho_v\right)+\nabla\bullet\left(\alpha_v\rho_v\vec{V}\right)=m \tag{5}$$

$$m=\frac{\rho_v\rho_l}{\rho_m}\frac{d\alpha_v}{dt} \tag{6}$$

where m is mass transfer rate.

On the ground of Rayleigh-Plesset equations and neglecting the second-order terms and the surface tension force, the following equation was obtained:

$$\frac{dR_B}{dt}=\sqrt{\frac{2}{3}\frac{p_v-p}{\rho_l}} \tag{7}$$

where p_v is the vapor pressure and set as 3540Pa corresponding to the vapor pressure of water at room temperature. Combining (4), (6) and (7), the algebraic expression of the source term m for the interphase mass transfer rate can be written as:

when $p_v>p$

$$m = \frac{\rho_v \rho_l}{\rho} \alpha_v (1-\alpha_v) \frac{3}{R_B} \sqrt{\frac{2}{3} \frac{(p_v - p)}{\rho_l}} \tag{8}$$

when $p_v \leq p$

$$m = \frac{\rho_v \rho_l}{\rho} \alpha_v (1-\alpha_v) \frac{3}{R_B} \sqrt{\frac{2}{3} \frac{(p - p_v)}{\rho_l}} \tag{9}$$

Additionally, the boundary condition was set as follows. The inlets of the primary and secondary flow both are mass flow inlet. The outlet boundary is pressure outlet. The axis is treated as axial symmetric boundary. The other boundary remained as wall. Through adjusting the outlet pressure, the different extent of cavitation in AJP can be obtained.

The time step is 5×10^{-5}s. The momentum equations and turbulent kinetic equations were discretized by a second-order upwind scheme and the SIMPLEC algorithm was applied to solve the coupling of the pressure and velocity. During calculating, the relative mass flow rate and the average total pressure at each inlet and outlet were monitored. If those parameters were hovering and fluctuating at a constant value and all residuals were lower than 1.0×10^{-5}, the calculation is considered convergent and the iteration was ceased.

2.2. CFD validation

In order to ensure the reliability of the simulation, the grid independence was confirmed firstly. And then the simulating result was compared with the experimental data from Shimizu [2]. The grid number was initially set as 50'000, and then increased to 200'000. In accord with the experimentation, the way to capture the cavitation flow during the validation was through increasing the total pressure of the primary flow. Fig. 3 indicates the comparison of the simulating result and the experimental data. As shown in the figure, the efficiency increases with the increasing q until it reaches the maximum value. Then the cavitation inception occurs and the efficiency begins to drop. If the total pressure of the primary flow keeps on increasing at this moments, the efficiency will decrease in pace with q.

After comparing the results from two sorts of grid in Fig. 3, it is obvious to find that they experience little differences and the grid number is independent. Moreover, both simulating results are basically in line with the experimental data. Consequently, it can be concluded that the result from this simulating strategy, with the grid number being 50'000, agreed well with the experimental data. And this strategy will be adopted in the following simulating.

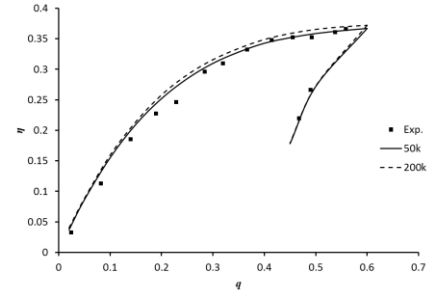

Fig. 3 Comparison of Experimental result and simulated result

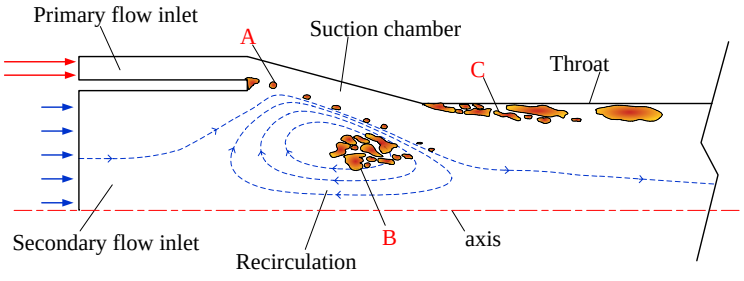

Fig. 4 Definition sketch of cavitation flow in AJP

3. Results and discussion

3.1. Flow pattern of cavitation in AJP

The flow in AJP is a sort of confined annular wall jet. The high pressure working flow was running adhering to the inner wall, so there is a separation of flow at the intersection of the suction chamber and the throat and cavitation is easy to be induced there. When AJP is working under relatively lower q, cavitation also forms at the shearing layer and the centre of the recirculation. Fig. 4 presents the definition sketch of cavitation flow in AJP and the region A, B and C represent the locations of

cavitation at the shearing layer, recirculation centre and throat inlet. In addition the bubble generated upstream joins together in the throat and collapses after encountering the high static pressure in the diffuser.

3.1.1. Cavitation at shearing layer

Cavitation at region A comprises of two scales: bubble-like and ribbon-like cavity. Fig. 5 shows the high speed snapshot of two kinds of cavity generating in shearing layer. The bubble-like cavity forms due to the small recirculation at the nozzle tip and the thickness of the nozzle tip determines the size of the bubbles. These bubbles sheds from the nozzle tip, stretches in shearing layer for the high shear force and then collapse into small micro bubbles. However, the ribbon-like cavity incepts at the shearing layer resembles small ribbons. The great velocity gradient at the shearing layer produces a large quantity of small vortices, the core of which become potential sites of cavitation for the pressure level drops. Additionally both of bubble-like and cloud like cavity see an apparent growth in the suction chamber due to the adverse pressure gradient.

3.1.2. Cavitation in the recirculation center

The cavitation at region B is mainly caused by the recirculation at the suction chamber. When the pump is working at a relatively low q, the fierce velocity gradient generates large recirculation at the axis of the suction chamber. Simultaneously the cavitation can consequently be induced at the centre of the recirculation. The lower the flow rate ratio is, the larger the recirculation area is and the easier the cavitation will be induced.

This kind of instable cavitation may mix with the bubbles forming in region A due to the entrainment effect of the recirculation. The stability of recirculation breaks subsequently. Fig. 6 presents a typical circle of the cavitation development in the recirculation under q=0.1. Apparently the cavity clouds at region *A* and *B* join together in Fig. 6 (c), grow in Fig. 6 (d) and fill the recirculation region in Fig. 6 (e). Finally the merged cavity cloud broke up Fig. 6 (f) and a new circle begins.

3.1.3. Cavitation induced at throat inlet

The cavitation at region C is mainly caused by the sudden change of the pump structure. Since the high velocity primary flow runs adhering to the inner wall, the flow separates at the intersection of the suction chamber and the throat. Then the following local low pressure leads to the cavitation inception and the bubbles develop in the throat as shown in Fig. 4.

As we decrease the outlet pressure, the cavitation at throat inlet experiences four stages, viz. incipient, stable, instable and fully developed stage. During this procedure, the pump efficiency gradually drops to zero until the flow is blocked in AJP.

Fig. 7 represents the incipient stages. A few bubbles form at throat inlet and collapse immediately. At this stage, the cavitation exerts little influences on the pump efficiency. The environmental pressure in the throat is still far higher than vapor pressure, so the pressure pulsation is insufficient to induce more intensive cavitation. As p_c decreases, the cavity cloud at throat inlet expands downstream and develops to a stable stage. Fig. 10 shows the time evolution of cavity cloud at the monitored window in Fig. 9 (corresponding to throat inlet) under the stable stage. The cavity length keeps constant accompanied with a slight fluctuation and the bubbles are much denser than that at the incipient stage. If p_c keeps on decreasing, the instable stage of the cavity cloud emerges. The time evolution of cavity cloud at the monitored window under instable stage is shown in Fig. 11. At this stage, the static pressure in the throat is approaching to the vapor pressure, and the cavity cloud adhering to the inner wall of the throat experiences a considerable fluctuation with the cavity length varying greatly, even extending to the diffuser. Note that the pump efficiency sees a sudden drop under this stage. When p_c decreases to a certain low value, the pump will work under operating limits with the pump efficiency decreasing to zero. Fig. 8 indicates a high speed snapshot of the fully developed cavity cloud at the throat inlet. At this time massive bubbles incept and develop in the throat, move to the diffuser and collapse after encountering the high static pressure. Since the main

flow is blocked thoroughly by the cavity cloud, the regulation of p_c only changes the length of the cavitation region and matters little on the flow condition in suction chamber.

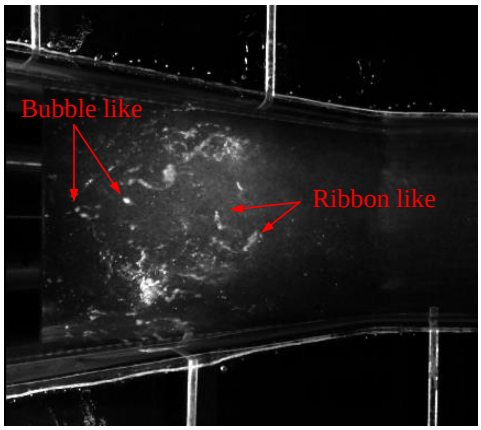

Fig. 5 High speed snapshot of two kinds of cavity generating in shearing layer

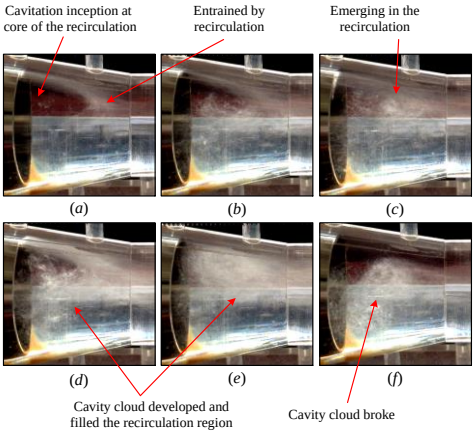

Fig. 6 Development of cavitation at recirculation center under low flow rate ratio (q=0.1)

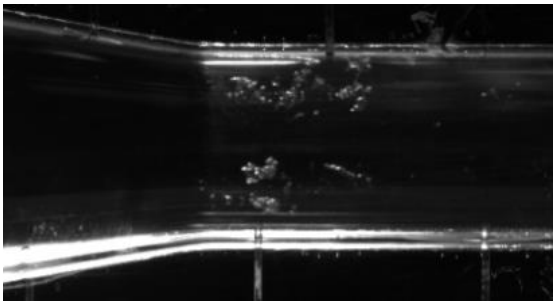

Fig. 7 High speed snapshot of cavitation at throat inlet under incipient stage

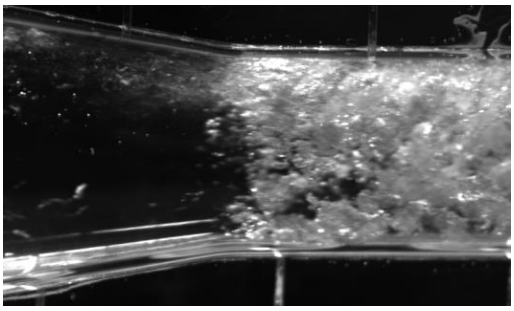

Fig. 8 High speed snapshot of fully developed cavity cloud at throat inlet

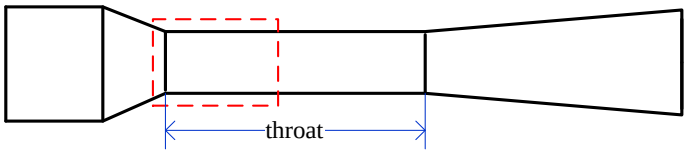

Fig. 9 the monitored window at throat inlet

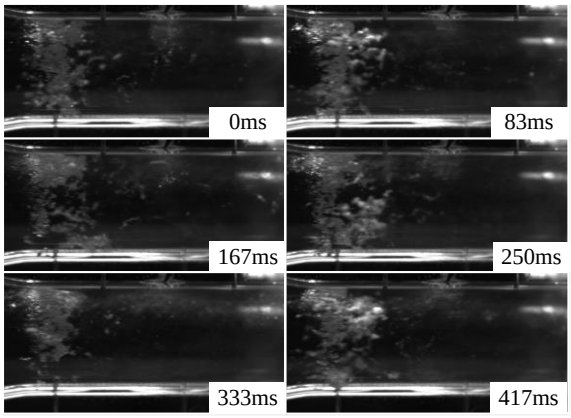

Fig. 10 Time evolution of cavity cloud at throat inlet under stable stage

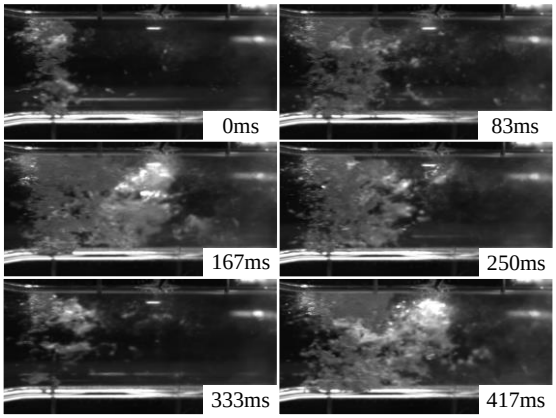

Fig. 11 Time evolution of cavity cloud at throat inlet under instable stage

3.2. Inner flow details

3.2.1. The recirculation in suction chamber

Recirculation is the most obvious flowing feature when AJP works under a certain low q. According to our previous investigation [11], the size of the recirculation varies inversely with the increasing q. and the recirculation vanishes when q increases to a certain value. The recirculation in the suction chamber is mainly determined by flow rate ratio and area ratio. However, the forming of cavitation in the suction chamber (corresponding to Region A and B in Fig. 4) greatly impacts on the size of the recirculation. Fig. 12 shows the time averaged vapor phase distribution and stream line in the suction chamber under different q and p_c. With p_c drops from 0.9kPa to 0.6kPa, the recirculation is apparently weakened by the growing cavity cloud. Especially when q=0.05 and p_c=0.6 or 0.7kPa, the recirculation is thoroughly broken by the fully developed cavity cloud. Moreover, the cavity cloud in the suction chamber tends to be fiercer when q is smaller. Since a smaller q causes a larger velocity gradient and adverse pressure gradient, the cavitation is more vulnerable at this time. As q=0.15, there are only a smaller cavity cloud at the shearing layer and the centre of the recirculation, which even cannot block the main flow.

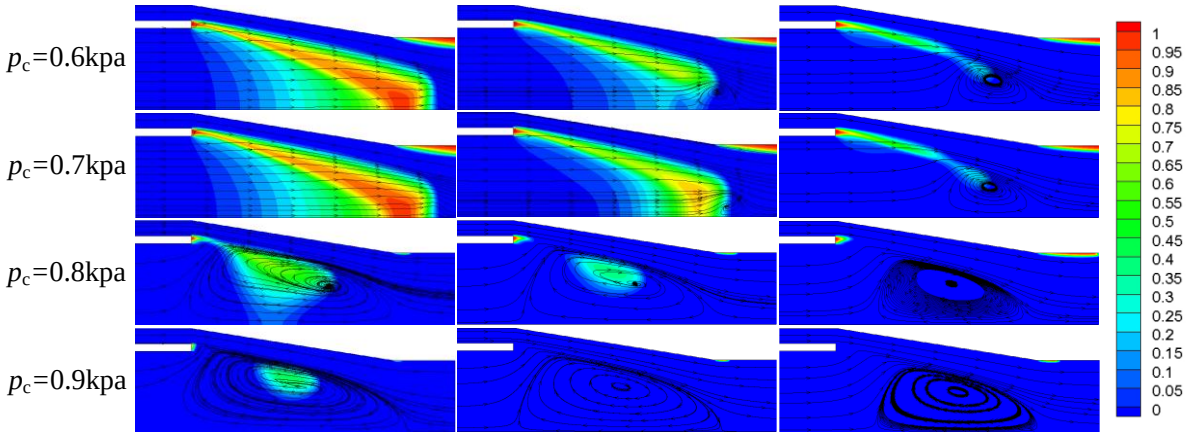

Fig. 12 Time averaged vapor phase distribution and streamline in suction chamber

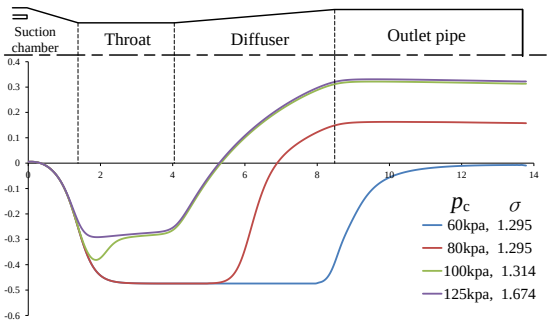

Fig. 13 C_p distribution along axis

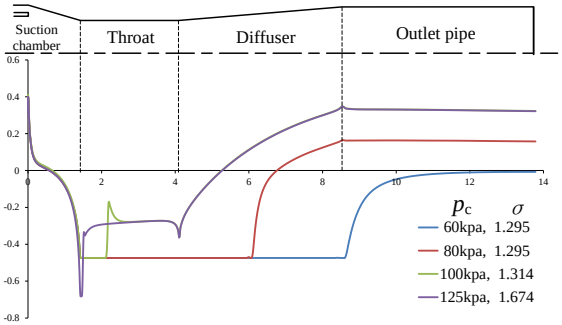

Fig. 14 C_p distribution along inner wall

3.2.2. Pressure coefficient distribution

In this work two dimensionless parameters, pressure coefficient C_p and cavitation number σ, were defined to analyse the flow inside AJP. Both of them can be calculated by the following equations,

$$C_p = \frac{p - p_0}{\frac{1}{2}\rho v_j^2} \tag{10}$$

$$\sigma = \frac{p_j - p_v}{\frac{1}{2}\rho\left(v_j - v_s\right)^2} \tag{11}$$

where p_v is the vapor pressure and p_j represents the static pressure at annular nozzle exit.

Fig. 13 presents C_p distribution along the axis under different outlet pressure when q=0.58. As shown in Fig. 13, C_p sees a smooth and stable increase in the throat when p_c=125kPa. However there is a significant adverse pressure gradient when p_c decreases to 100kPa. As p_c drops to 80kPa, the throat is filled with bubbles and the local static pressure in the throat equals the vapor pressure. At this time the pump efficiency decreases to zero and the cavitation number σ declines to its minimum value correspond to q=0.58. This value is denoted as the critical cavitation number σ_c in this paper and a larger σ_c mean cavitation is easy to be induced in AJP and the cavitation performance is worse. More detail on σ_c will be presented in the following section.

Fig. 14 shows C_p distribution along the inner wall corresponding to the working condition in Fig. 13. A same trend of C_p distribution in Fig. 13 and Fig. 14 is obtained. However with regard to the case of p_c=100kPa and σ=1.314, C_p at the inner wall reaches to the minimum pressure (the vapor pressure) earlier than that on the axis. According to the previous investigation, the incipient cavitation is adhering to the inner wall of the throat. With the decreasing p_c, the cavitation region expands upstream and the thickness increases as well. Hence the low pressure region firstly forms at the inner wall and then extends to the axis.

3.3. Cavitation performance

According to the theory of central jet pump and Shimizu's derivation on AJP pump performance, the energy efficiency of AJP can be expressed as follow:

$$\eta = q \bullet h = \frac{Q_s}{Q_j}\frac{P_c - P_s}{P_j - P_c} \tag{11}$$

where h is the pressure ratio, P represents the total pressure at any cross section and the subscript j, s and c represents the cross section at annular nozzle exit, the suction pipe exit and the outlet of diffuser respectively.

Fig. 15 (a), (b) and (c) indicate the pump efficiency versus cavitation number σ under different flow rate ratio. For each constant q, η keeps constant regardless of the decreasing σ until that cavitation emerges in AJP and σ declines to a certain value (the critical cavitation number σ_c as mentioned in section 3.2.2). Then η experiences a sudden drop.

Moreover, q impacts a lot on η and σ_c. When q<0.2 as shown in Fig. 15 (a), η under no cavitation condition greatly increases with the increasing q, while σ_c varies little and η for each q drops to zero at a same σ. Since the cavitation at shearing layer and the centre of the recirculation in suction chamber plays a main role on blocking the secondary flow under a considerably low q, the primary flow consequently consumes little momentum on entraining the secondary flow. Thus σ_c keeps constant when q<0.2. However as q ranging from 0.2 to 0.65, σ_c is proportional to q as shown in Fig. 15 (b) and (c). The cavitation in the suction chamber disappeared (Region A and B in Fig. 4), while the cavitation adhering to the inner wall of the throat (Region C in Fig. 4) mainly influences the pump efficiency. Hence the more momentum the primary flow costs on entraining the secondary flow, the cavitation is easier to be induced in the throat. When 0.5≤q≤0.65, η varies little and hovers around 35%. This section of q is corresponding to maximum working condition, while AJP are more vulnerable to cavitation on this condition.

Combined Fig. 15 (a), (b) and (c) together, we obtained the envelop line of η and σ_c under critical cavitation condition in Fig. 15 (d). According to the envelop line, the relationship between σ_c and q can be divided into two part. When σ_c<0.31, it keeps constant regardless of q, while it increases linearly with the increasing q when ranging from 0.31 to 1.58.

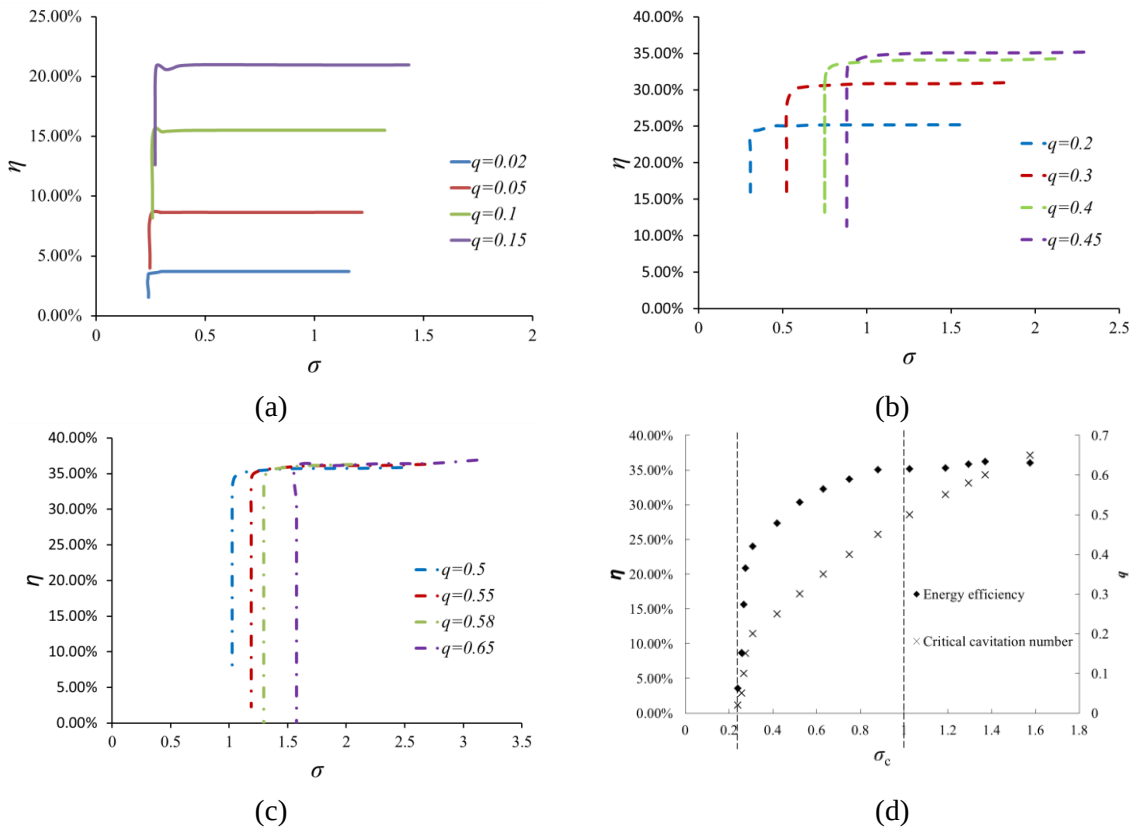

Fig. 15 (a), (b) and (c): η versus σ under different q; (d): Envelop line of η under critical cavitation condition

4. Conclusion

In this work high speed imaging method and numerical method were adopted to study the cavitation flow in annular jet pump under different flow rate ratio. The cavity cloud induced at different places in AJP under different flow condition was analysed in details. Furthermore the cavitation performance and the inner flow details are also analysed on the ground of CFD method. The following conclusions are obtained.

- k-ε turbulence model combined with Mixture model and Schnerr-Sauer model is suitable to predict the variation of pump efficiency under different q including cavitation and no cavitation working condition.
- Cavitation in AJP can be induced at the shearing layer, the centre of the recirculation and the throat inlet. The cavity in the recirculation tends to merge with the bubbles generating at the shearing layer and break the recirculation periodically. The cavitation at throat inlet experiences four stages, incipient, stable, instable and fully developed stage. The first two stages impact little on pump efficiency and the instable stage sees a low frequency fluctuation. As the cavitation in the throat fully developed, the main flow in AJP is blocked and the pump efficiency drops suddenly.
- When q<0.2, the cavitation at the shearing layer and the centre of the recirculation greatly affects the flow condition in AJP. The recirculation is significantly weakened by the growing cavitation in the suction chamber with the decreasing outlet pressure. Moreover, the critical cavitation number is below 0.31 and varies little with the flow rate ratio.
- When q>0.2, the cavitation induced at the throat inlet plays an important role on pump efficiency. With the decreasing outlet pressure, the cavity adhering to the inner wall of the throat extends downstream, even to the diffuser and the thickness of the cavity cloud increases

as well. The critical cavitation number is proportional to the flow rate ratio and sees a linear relationship with the increasing q.

Nomenclature

A_{so}	cross sectional area of suction pipe	v	axial velocity
D_0	diameter of outlet pipe	α	angle of suction chamber
D_t	diameter of throat	β	angle of diffuser
D_{so}	inner diameter of suction pipe	η	AJP pump efficiency
C_p	pressure coefficient $C_p=(p-p_0)/(\rho u_j^2/2)$	ρ_l	density of liquid
P	total pressure	ρ_v	density of vapor
p	static pressure	ρ_m	density of mixture
p_v	static pressure at suction duct exit	σ	cavitation number
p_0	static pressure at suction duct exit	σ_c	critical cavitation number
Q	volume flow rate		
q	flow rate ratio Q_s/Q_j	Subscript:	
L_c	length of suction chamber	j	primary flow at nozzle exit
L_t	length of throat	s	entrained secondary flow at suction duct
m	Area ratio A_{th}/A_j	c	mixed flow at diffuser outlet

Acknowledgments
This research is financially supported by the National Natural Science Foundation of China under the Contract No. 51179134, National Key Basic Research Program of China (NO. 2014CB239203) and New Century Excellent Talents in University (NCET-12-0424).

Reference

[1] Shimizu Y and Kuzuhara S 1983, *2nd Int. Conf. on Cavitation.* 77-81.
[2] Shimizu Y, Nakamura S, Kazuhara S and Kurata S 1987 *ASME J.Fluids Eng*. **109**(3) 205-212.
[3] Elger D F, Taylor S J and Liou C P 1994 *ASME J.Fluids Eng*. **166**(4) 735–740.
[4] Long X,Yan H, Zhang S and Yao X 2010 *J.Drainage Irrigation Machinery Eng.* **28**(3) 198-201
[5] Lu H and Shang H 1987 *SCIENTIA SINICA.* **30**(11) 1174 – 1187.
[6] Kudirka A A and Decoster M A 1979 *ASME J. Fluids Eng.* **101**(1) 93–99
[7] Wiesche S 2005 *Heat Mass Transfer.* **41**(7) 615 - 624.
[8] Long X, Yao H and Zhao J 2009 *Int. J. Heat Mass Transfer*. **52**(9) 2415-2420.
[9] Ran B and Katz J 1994 *J. Fluid Mech.* **262** 223-263.
[10] Long X, Cheng Q, Han N, Cai B and Wang F 2010 *J. Drainage Irrigation Machinery Eng.* **28**(1) 001
[11] Xiao L, Long X, Li X, et al. 2013 *J. Mechanical Sci. Technol.* **27**(6) 1603-1609.